The Journal of Immunology

# Inflammatory Responses to Pneumovirus Infection in IFN- αβR Gene-Deleted Mice

Tara L. Garvey, Kimberly D. Dyer, John A. Ellis, Cynthia A. Bonville, Barbara Foster, Calman Prussin, Andrew J. Easton, Joseph B. Domachowske and Helene F. Rosenberg

*J Immunol* 2005; 175:4735-4744; ;
doi: 10.4049/jimmunol.175.7.4735
http://www.jimmunol.org/content/175/7/4735



*The Journal of Immunology* is published twice each month by
The American Association of Immunologists, Inc.,
1451 Rockville Pike, Suite 650, Rockville, MD 20852

Print ISSN: 0022-1767 Online ISSN: 1550-6606.

# Inflammatory Responses to Pneumovirus Infection in IFN-$\alpha\beta$R Gene-Deleted Mice[1]

**Tara L. Garvey,* Kimberly D. Dyer,* John A. Ellis,† Cynthia A. Bonville,‡ Barbara Foster,* Calman Prussin,* Andrew J. Easton,§ Joseph B. Domachowske,‡ and Helene F. Rosenberg[2]***

**Pneumonia virus of mice (PVM; family *Paramyxoviridae*) is a natural pathogen of rodents that reproduces important clinical features of severe respiratory syncytial virus infection in humans. As anticipated, PVM infection induces transcription of IFN antiviral response genes preferentially in wild-type over IFN-$\alpha\beta$R gene-deleted (IFN-$\alpha\beta$R$^{-/-}$) mice. However, we demonstrate that PVM infection results in enhanced expression of eotaxin-2 (CCL24), thymus and activation-regulated chemokine (CCL17), and the proinflammatory RNase mouse eosinophil-associated RNase (mEar) 11, and decreased expression of monocyte chemotactic protein-5, IFN-$\gamma$-inducible protein-10, and TLR-3 in lung tissue of IFN-$\alpha\beta$R$^{-/-}$ mice when compared with wild type. No differential expression of chemokines MIP-1$\alpha$ or MIP-2 or Th2 cytokines IL-4 or IL-5 was observed. Differential expression of proinflammatory mediators was associated with distinct patterns of lung pathology. The widespread granulocytic infiltration and intra-alveolar edema observed in PVM-infected, wild-type mice are replaced with patchy, dense inflammatory foci localized to the periphery of the larger blood vessels. Bronchoalveolar lavage fluid from IFN-$\alpha\beta$R$^{-/-}$ mice yielded 7- to 8-fold fewer leukocytes overall, with increased percentages of eosinophils, monocytes, and CD4$^+$ T cells, and decreased percentage of CD8$^+$ T cells. Differential pathology is associated with prolonged survival of the IFN-$\alpha\beta$R$^{-/-}$ mice (50% survival at 10.8 ± 0.6 days vs the wild type at 9.0 ± 0.3 days; $p < 0.02$) despite increased virus titers. Overall, our findings serve to identify novel transcripts that are differentially expressed in the presence or absence of IFN-$\alpha\beta$R-mediated signaling, further elucidating interactions between the IFN and antiviral inflammatory responses in vivo.** ***The Journal of Immunology,*** **2005, 175: 4735–4744.**

The actions of type I IFNs promote host defense against virus infections of all types, and are best known for their role in inducing the synthesis of antiviral IFN-response genes (reviewed in Refs. 1, 2). Viruses have developed a variety of anti-IFN strategies; viruses of the family *Paramyxoviridae*, the subject of this work, have developed mechanisms that involve interactions with virus accessory proteins that ultimately block IFN-mediated intracellular signaling pathways (reviewed in Refs. 3–6). Paramyxoviruses of the subfamily *Pneumovirinae*, which include the pathogens human and bovine respiratory syncytial viruses (hRSV[3]; bRSV) have distinct anti-IFN mechanisms; they do not limit IFN production, nor do they interfere with receptor binding or signal transduction. Several groups have presented evidence suggesting that the bRSV and hRSV nonstructural NS1 and NS2 proteins in some way antagonize the IFN-induced antiviral state (7–10).

Of particular recent interest are the ways in which IFNs and IFN-mediated signaling mechanisms interact with proinflammatory pathways and modulate the production of chemoattractant cytokines. Among the responses that have been studied thus far, the transcriptional activator, IFN-response factor (IRF)-3 is an absolute requirement for the production of the CC chemokine, RANTES, in response to infection with the paramyxoviruses Sendai (11, 12) or hRSV (13) in tissue culture. Interestingly, RANTES was not detected in a gene microarray study designed to identify gene transcription in vitro in response to overexpression of IRF-3 alone in the absence of virus infection (14); neither were any proinflammatory chemokine transcripts detected in a microarray study designed to evaluate responses to IRF-5 and IRF-7 (15). At the same time, intriguing relationships between inflammatory responses to virus infection and interactions with IFN-$\gamma$ have been described (16–18).

Pneumonia virus of mice (PVM) is a virus of the family *Paramyxoviridae*, subfamily *Pneumovirinae*, and is the only pathogen of this subfamily that includes mice as its natural host. Intranasal inoculation with as few as 10–30 PFU of the mouse-passaged J3666 strain of PVM results in severe respiratory virus infection with robust replication to $10^8$ PFU/g lung, accompanied by an inflammatory response mediated at least in part by the actions of the chemokine MIP-1$\alpha$ and its signaling through its major receptor CCR1 on granulocytes. Unless mice are treated with both antiviral (ribavirin) and immunomodulatory therapies (anti-MIP-1$\alpha$ or anti-CCR1) (19, 20), virus replication and the ensuing granulocytic inflammatory response lead to the significant morbidity and mortality. PVM has also been shown to be an important model for the study of postvirus Th2 responses (21).

*Laboratory of Allergic Diseases, National Institute of Allergy and Infectious Diseases, National Institutes of Health, Bethesda, MD 20892; †Western College of Veterinary Medicine, Saskatoon, Saskatchewan, Canada; ‡State University of New York, Upstate Medical University, Syracuse, NY 13210; and §Department of Biological Sciences, University of Warwick, Coventry, United Kingdom

Received for publication April 6, 2005. Accepted for publication July 18, 2005.

The costs of publication of this article were defrayed in part by the payment of page charges. This article must therefore be hereby marked *advertisement* in accordance with 18 U.S.C. Section 1734 solely to indicate this fact.

[1] This work was supported by National Institute of Allergy and Infectious Diseases, Division of Intramural Research (to H.F.R.), and a Scientist Development grant from the American Heart Association (to J.B.D.).

[2] Address correspondence and reprint requests to Dr. Helene F. Rosenberg, Building 10, Room 11N104, National Institute of Allergy and Infectious Diseases, National Institutes of Health, 9000 Rockville Pike, Bethesda, MD 20892. E-mail address: hrosenberg@niaid.nih.gov

[3] Abbreviations used in this paper: hRSV, human respiratory syncytial virus; bRSV, bovine respiratory syncytial virus; IRF, IFN-response factor; PVM, Pneumonia virus of mice; IP, IFN-induced protein; TARC, thymus and activation-regulated chemokine; MDC, macrophage-derived chemokine; Q-RT-PCR, quantitative RT-PCR.



0022-1767/05/$02.00

In this work, we study the pathogenesis of PVM infection in mice devoid of the receptor for type I IFNs (IFN-$\alpha\beta$R gene-deleted (IFN-$\alpha\beta R^{-/-}$) mice; Ref. 21), and we identify a group of proinflammatory mediators whose expression is modulated (directly or indirectly) by IFN receptor-mediated signaling. The differential expression of these mediators is accompanied by differential pathology and cellular inflammation in response to this respiratory virus infection.

## Materials and Methods

### *IFN-$\alpha\beta R^{-/-}$ gene-deleted mice*

IFN-$\alpha\beta R^{-/-}$ mice (22) (C57BL/6 background) were generated from heterozygotes and identified by standard PCR of genomic DNA isolated from tailsnips (primer sequences: sense UM4, 5′-AAGATGTGCTGTTCCCT TCCTCTGCTCTGA-3′; antisense UM5, 5′-AAGATGTGCTGTTCCCT TCCTCTGCTCTGA-3′ (150-bp band from wild-type allele only); Neo sense, 5′-TCAGCGCAGGGGCGCCCGGTTCTTT-3′; and Neo antisense, 5′-TCAGCGCAGGGGCGCCCGGTTCTTT-3′ (340-bp band from Neo cassette only).

### *Inoculation with PVM*

Virus stocks (PVM strain J3666 at $10^6$ PFU/ml) were prepared from mouse lung homogenates, and titers were determined as described previously (23). Mice were anesthetized briefly via inhalation of 20% halothane solution and, unless otherwise indicated, inoculated intranasally with 60 PFU PVM (strain J3666) in a 50- to 80-$\mu$l volume with IMDM as diluent. Mice were sacrificed at time points indicated by gentle cervical dislocation. All of the procedures were reviewed and approved by the National Institute of Allergy and Infectious Diseases Animal Care and Use Committee per animal study protocol LAD-8E.

### *Microscopic histology*

Lungs for histology were inflated transtracheally with 0.2–0.3 ml of ice-cold phosphate-buffered 10% formalin before excision and fixation in same. Paraffin blocks, slide preparation, and H&E staining were done commercially (American Histolabs). Three slides each from three individual mice of each genotype (wild-type IFN-$\alpha\beta R^{+/+}$ and gene-deleted IFN-$\alpha\beta R^{-/-}$) at three distinct time points (total 54 slides) were coded by one investigator and assessed in that form by the veterinary pathologist (J. A. Ellis) to assure an unbiased reading.

### *Bronchoalveolar lavage fluid and cell differentials*

Lungs were inflated transtracheally with cold 0.8 ml of PBS + 0.1% BSA + 1 mM EDTA, repeated once for a recovered volume of 1.5 ml. Cytospin preparations (100 $\mu$l per slide; Thermo Shandon) were prepared and stained with DiffQuik (Fisher Scientific) for leukocyte differential counts. One hundred to 200 hundred cells were scored per slide; $n = 3$–4 mice per point.

### *Preparation of mouse lung tissue homogenates and RNA*

For analysis of protein, lung tissue was immersed in 1 ml of cold IMDM and subjected to blade homogenization. Tissue debris was removed by centrifugation at 4°C, and clarified supernatant was frozen on dry ice-ethanol and stored at −80°C before analysis. For analysis of RNA, mouse lung was immersed in 3–4 ml of RNAlater (Ambion), stored overnight at 4°C, then at −80°C until use. For preparation of RNA, samples were defrosted at room temperature, and lung tissue was removed from RNAlater, immersed in 5 ml of RNAzol, and processed as described previously (24).

### *Western blots*

Clarified homogenates of mouse lung tissue (6 mg protein/ml) were diluted 1/1 in reducing sample buffer, heated to 65°C for 5 min and subjected to electrophoresis on 14% Tris-glycine SDS acrylamide gels and transfer to nitrocellulose membranes by standard methods. Membranes were probed with either 1) 1/500 dilution of rabbit polyclonal anti-PVM N protein antiserum or 2) 1/300 dilution of rabbit polyclonal anti-mouse eosinophil-associated RNase (mEars) antiserum, followed by a 1/1000 dilution of alkaline-phosphatase-linked goat anti-rabbit IgG and standard developing reagents (25).

### *ELISAs*

ELISAs (R&D Systems) were performed to detect IFN-$\alpha$, MIP-1$\alpha$, MIP-2, thymus and activation-regulated chemokine (TARC), macrophage-derived chemokine (MDC), IL-4, IL-5, monocyte chemotactic protein-5, IFN-induced protein (IP)-10, and IFN-$\beta$, per manufacturer's instructions. Protein concentrations were determined by BCA assay (Pierce).

### *RNase assay*

The RNase assay is essentially as described (25). Twenty microliters of mouse lung homogenate were added to 0.8 ml of 40 mM sodium phosphate (pH 7.4), all maintained at room temperature. The reaction was initiated with the addition of 10 $\mu$l of a stock of 20 mg/ml tRNA (Sigma-Aldrich), and reaction stopped at t = 20 min by the addition of ice-cold 20 mM lanthanum nitrate and 3% perchloric acid. A t = 0 spectrophotometric blank was prepared by adding stop solution to the buffer and RNase mix before addition of tRNA. Acid insoluble substrate (polymeric tRNA) was separated from acid soluble product (ribonucleotides) by centrifugation. Data obtained were corrected for total protein concentration as determined by BCA assay.

### *Gene microarray*

Gene microarray was performed on lung RNA from PVM-infected and sham (diluent control)-inoculated mice sacrificed on day 6 postinoculation. All of the microarray procedures were conducted at the Microarray Core Facility (Rochester, NY) as described in our previous publication (24). This study used the M430 mouse gene microarray chip (Affymetrix) and was analyzed using GeneSpring 6.1 Software (Silicon Genetics).

### *Quantitative RT-PCR (Q-RT-PCR)*

RNA samples (5 $\mu$g each) from three to five mice were pooled and treated with RNase-free DNase I (Invitrogen Life Technologies) before reverse transcription (1st strand synthesis kit; Roche Diagnostics) to cDNA. All of the reactions include reverse-transcriptase negative controls. Reactions for detection of the GAPDH housekeeping gene or the PVM virus SH gene include the ABI TaqMan reagent (×1) (Applied Biosystems), 100 nM primers (see below), 200 nM probe, 2 $\mu$l of cDNA template generated by reverse transcription step above, and distilled water to 25 $\mu$l. Primers and probes were as follows: rodent GAPDH set, Vic-labeled probe, (ABI catalog no. 4308313); PVM SH set, probe 5′-6FAM-CGCTGATAATGGC-CTGCAGCA TAMRA-3′, primer 1, 5′-GCCTGCATCAACACAGT-GTGT-3′; primer 2, 5′-GCCTGATGTGGCAGTGCTT-3′. Reactions to detect all other genes described included ×20 concentrated primer probe sets designed by ABI Assay by Design, which were diluted in the reaction mixture per manufacturer's instructions. Primers and probes from ABI as follows: mEar11, Mm00519056_s1; Infb, Mm00439546_s1; CCL24, Mm00111701_m1; Oas1b, Mm00449297_m1; Oas3, Mm00460944_m1; Mx1, Mm00487796_m1; TLR3, Mm00446577_g1; Oas1g, Mm00726868_s1; and Oas2, Mm00460961_m1. Reactions were performed in an ABI 7700 Sequence detector,50°C for 2 min, 95°C for 10 min, followed by 40 cycles of 95°C for 15 s and 60°C for 1 min. Data were normalized to GAPDH expression, and statistical significance was determined using the *t* test assuming equal variance.

### *Flow cytometric analysis*

Total cells from BAL fluid from wild-type (IFN-$\alpha\beta R^{+/+}$) and IFN-$\alpha\beta R^{-/-}$ mice on day 6 postinoculation were stained with the following mAb-fluorochrome conjugates: CD3 FITC, CD4 PE, CD8 allophycocyanin, and I-$A^b$ PE/Cy5 (all from BD Pharmingen) in PBS with 0.1% BSA for 30 min. After staining, cells were washed twice in PBS with 0.1% BSA, stained with propidium iodide, and analyzed by flow cytometry. Control samples were stained with isotype-matched mAbs replacing CD4 and CD8. Each mouse BAL sample was analyzed individually. Data were acquired with a 2-laser, 4-parameter FACSCalibur flow cytometer (BD Biosciences) and analyzed on CellQuest software (BD Biosciences). Viable T cells were identified by first gating on cells of typical lymphocyte forward and side scatter, followed by gating on $CD3^+$, I-$A^b$-negative, propidium iodide-negative cells. CD4 vs CD8 dot plots were generated, and the frequency of each subpopulation was determined. Quadrant statistical markers were placed on the basis of the isotype-matched controls. Typically, 50,000–200,000 total events were acquired to obtain 1,500–4,500 T cells per sample.

### *Statistical analysis*

Statistical analysis was performed using Student's *t* test or Mann-Whitney *U* test as appropriate.

## Results

### *Identification of transcripts preferentially expressed in PVM-infected, wild-type vs IFN-αβR-deficient mice*

We performed gene microarray analysis comparing transcripts expressed in PVM-infected wild-type (IFN-$\alpha\beta R^{+/+}$) mice to those expressed in PVM-infected gene-deleted (IFN-$\alpha\beta R^{-/-}$) mice at day 6 postinoculation. The initial half of the microarray analysis, which lists transcripts preferentially expressed in the PVM-infected wild-type mice, is shown in Table I. Most prominent among these preferentially expressed transcripts are the classic IFN response genes: the IFN-induced proteins with tetratricopeptide repeats, the IFN-activated genes 203 and 204, IFN regulator factor 7, Stat 2, and the antiviral IFN response genes, including the 2′-5′ oligoadenylate synthetases, RNA-dependent protein kinase, and myxovirus resistance 1 gene, the latter set confirmed by Q-RT-PCR and shown in Fig. 1. TLR-3 (Fig. 1), the dsRNA receptor, previously identified as an IFN response gene by Heinz et al. (26), is also preferentially expressed in the wild-type mice, as is ubiquitin-specific protease 18 (also known as UBP43), which specifically removes the IFN-stimulated protein, ISG15, from intracellular protein conjugates (27). Two other transcripts that were preferentially expressed in the wild-type mice, those encoding ubiquitin-specific protease 1 (+36-fold) and RNA binding motif 11 (+17-fold), have no previously recorded relationship to IFN receptor-mediated signal transduction, and may bear some unique relationship to this experimental circumstance.

### *Preferential expression of chemokines monocyte chemotactic protein-5 and IP-10 in wild-type (IFN-αβR$^{+/+}$) mice*

Monocyte chemotactic protein-5 (CCL-12) is produced in macrophages, smooth muscle cells, and mast cells and is an agonist for the receptor CCR2. The gene microarray results indicate a 3.3-fold increase in transcript encoding monocyte chemotactic protein-5 in PVM-infected wild-type lung tissue as compared with wild type on day 6 postinoculation. This finding is confirmed at the level of immuoreactive protein by ELISA (Table II).

Differential expression of IP-10 (CXCL-10) was detected at only 2.8-fold on gene microarray (Table I). However, we observed

Table I. *Differential expression of transcripts comparing pneumovirus-infected wild-type vs. IFN-αβR gene-deleted mice*[a]

| Accession No. | Gene | Description | Fold Change |
|---|---|---|---|
| Antiviral IFN response genes | | | |
| BE11144 | *PRKR* | RNA-dependent protein kinase | +3.23 |
| AB067535 | *Oas2* | 2′–5′oligoadenylate synthetase 2 | +3.66* |
| BC018470 | *Oas1g* | 2′–5′oligoadenylate synthetase 1G | +4.81* |
| BQ033138 | *Oasl2* | *Mus musculus* sequelae homologous to Oas like | +4.87 |
| AB067533 | *Oasl1* | 2′–5′oligoadenylate synthetase-like 1 | +6.43* |
| AB067534 | *Oas3* | 2′–5′oligoadenylate synthetase 3 | +13.78* |
| M21039 | *Mx1* | Myxovirus (influenza virus) resistance 1 | +19.28* |
| TLR | | | |
| NM_126166 | *TLR-3* | TLR-3 | +5.78* |
| Type I IFN and IFN signaling | | | |
| NM_010502 | *Ifna1* | IFN-α1 | +2.63** |
| NM_010503 | *Ifna2* | IFN-α2 | +0.63 |
| NM_010504 | *Ifna4* | IFN-α4 | +1.13 |
| NM_010505 | *Ifna5* | IFN-α5 | +1.72 |
| NM_008334 | *Ifna7* | IFN-α7 | +1.13 |
| NM_008335 | *Ifna8* | IFN-α8 | +0.62 |
| NM_010507 | *Ifna9* | IFN-α9 | +1.11 |
| NM_008333 | *Ifna11* | IFN-α11 | +1.35 |
| NM_010510 | *Ifnb* | IFN-β | +1.12* |
| BB030134 | *Stat2* | Signal transducer and activator of transcription 2 | +2.94 |
| IFN-stimulated genes | | | |
| NM_008328 | *Ifi203* | IFN-activated gene 203 | +3.63 |
| NM_008331 | *Ifit1* | IFN-induced protein w/ tetratricopeptide repeats 1 | +5.13 |
| NM_010501 | *Ifit3* | IFN-induced protein w/ tetratricopeptide repeats 3 | +5.85 |
| NM_008329 | *Ifi204* | IFN-activated gene 204 | +6.66 |
| NM_016850 | *Irf7* | IFN regulatory factor 7 | +6.73 |
| NM_008332 | *Ifit2* | IFN-induced protein w/ tetratricopeptide repeats 2 | +9.73 |
| Inflammation related proteins | | | |
| U50712 | *CCL12* | Macrophage chemoattractant protein-5, CC chemokine ligand 12 | +3.33* |
| NM_013542 | *Gzmb* | Granzyme B | +6.25 |
| AK004595 | *Tyki* | LPS-inducible thymidylate kinase | +7.70 |
| BC027310 | *Fcrl3* | Fc receptor-like 3 (CD16–2) | +3.31 |
| AF143181 | *Fcgr1* | High-affinity Fc receptor (CD64) | +5.67 |
| NM_013377 | *CCL3* | MIP-1α | +2.09* |
| NM_009140 | *CXCL2* | Macrophage inflammatory peptide-2 | +1.32* |
| NM_021274 | *CXCL10* | IP-10 | +2.81* |
| NM_013653 | *CCL5* | RANTES | +2.36 |
| Other | | | |
| AI987929 | *Ndr1* | N-*myc* downstream regulated 1 | +4.20 |
| AV272221 | *Rbm11* | RNA binding motif protein 11 | +17.19 |
| C79248 | *RNpc2* | RNA binding region containing 2 | +3.09 |
| BQ033290 | *Usp1* | Ubiquitin-specific protease 1 | +35.58 |
| NM_011909 | *Usp18* | Ubiquitin-specific protease 18 | +5.30 |

[a] Only values ≥ 2.5 are considered significant. Values denoted by asterisks (*) have been evaluated by QRT-PCR and/or ELISA; the IFN-α were evaluated as a group by ELISA (**).

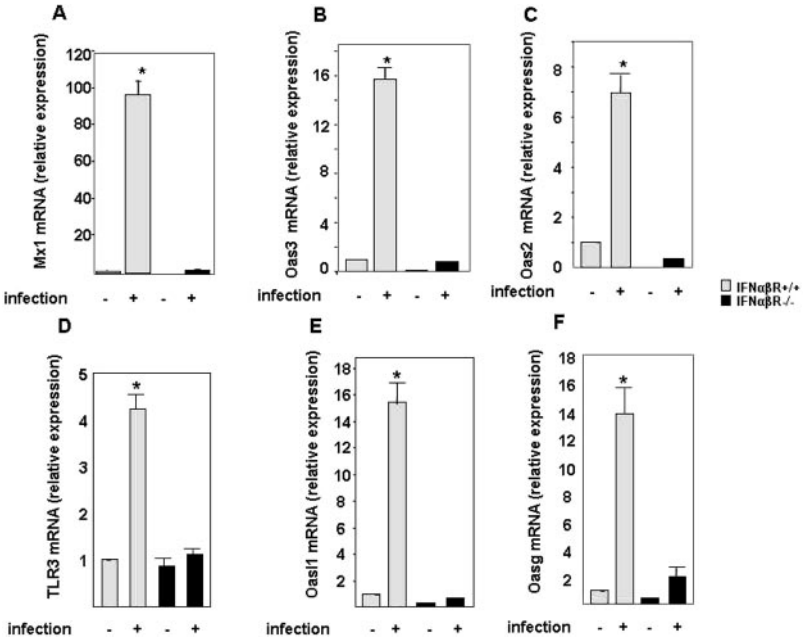


**FIGURE 1.** Relative expression of transcripts encoding IFN response genes *Mx1* (*A*), *Oas3* (*B*), *Oas2* (*C*), *TLR3* (*D*), *Oasl1* (*E*), and *Oasg* (*F*) in total RNA isolated from whole lungs from mice inoculated with 60 PFU PVM on day 0 (infection −) and sacrificed on day 6 postinoculation (infection +), confirming results of gene microarray analysis (see Table I; $n = 4$–5 mice per time point). Genotypes, IFN-αβR$^{+/+}$ and IFN-αβR$^{-/-}$ mice. Asterisks (*) denote statistically significant differences (*, $p < 0.01$) between datapoints indicated and others shown.

profound differential expression of this proinflammatory mediator in lung tissue with 5- to 10-fold greater expression detected in lungs of wild-type as compared with IFN-αβR-deficient mice (Table II). Reduction in the synthesis of IP-10 may be related to the reduced expression of TLR3 observed among IFN-αβR-deficient mice; Rudd et al. (28) demonstrated that targeted disruption of TLR3 expression by small interfering RNA resulted in reduced expression of IP-10 in response to hRSV in the MRC-5 fibroblast cell line.

Targeted disruption of TLR3 also resulted in reduced expression of RANTES (CCL5) in response to hRSV infection in the MRC-5 cell line (28), and we observed a 2.36-fold greater expression of RANTES transcript in the wild-type mice. However, no differential expression of immunoreactive protein was observed in lung tissue, potentially due to the high levels of RANTES present at baseline in uninfected mouse lung tissue (data not shown).

### *Expression of type I IFNs in wild-type and IFN-αβR$^{-/-}$ mice*

We evaluated the production in both wild-type and IFN-αβR$^{-/-}$ mice in response to PVM infection (Fig. 2). Immunoreactive IFN-α was detected by ELISA in uninfected wild-type and IFN-αβR$^{-/-}$ mice, and PVM infection resulted in a significant (3.6-fold) increase to 99.1 ± 24 pg/ml/mg protein in wild-type mice. In contrast, PVM infection resulted in a statistically significant but comparatively minimal increase in IFN-α production (1.6-fold, to 37.8 ± 6.9 pg/ml/mg protein) in the IFN-αβR$^{-/-}$ gene-deleted mice. The majority of the differential expression appears to be from the Ifna1 gene locus (Table I), although it would be necessary to sequence a statistically significant number of gene transcripts to confirm this. The differential expression of type I IFNs in response to infection is similar to that described by Malmgaard et al. (29) in their study of these mice infected with lymphocytic choriomeningitis virus in IFN-αβR$^{-/-}$ mice.

Similarly, we observed a 23 ± 6-fold increase in relative expression of mRNA encoding IFN-β in wild-type mice, as compared with a 1.5 ± 0.3-fold increase among IFN-αβR$^{-/-}$ mice. However, this degree of differential expression was not apparent in the gene array or on immunoassay of lung homogenate or BAL fluid, both of which contained minimal levels of immunoreactive IFN-β (<50 pg/ml throughout). Although this is not inconsistent with our quantitative PCR results (Fig. 2), because this method can detect very small amounts of differentially expressed mRNA, one must conclude that IFN-β is probably not contributing as much as IFN-α to the responses observed.

Table II. *Detection of monocyte chemotactic protein-5 in lung tissue homogenates and detection of CXCL10 in lung tissue homogenates and BAL fluid of wild-type (IFN-αβR$^{+/+}$) and IFN- αβR gene-deleted mice (IFN-αβR$^{-/-}$) in response to infection with PVM (inoculation on day 0 with 60 PFU)*[a]

| | IFN-αβR$^{+/+}$ | IFN-αβR$^{-/-}$ |
|---|---|---|
| Monocyte chemotactic protein-5 (CCL-12; pg/ml/mg lung homogenate protein) | | |
| Day 0 | 0 | 0 |
| Day 3 | 31.0 ± 7.7 | 27.0 ± 7.9 |
| Day 4 | 92.0 ± 14 | 15.2 ± 7.1* |
| Day 5 | 375 ± 106 | 16.3 ± 4.9* |
| Day 6 | 602 ± 150 | 151 ± 37* |
| IP-10 (CXCL-10; pg/ml mg lung homogenate protein) | | |
| Day 6 | 4490 ± 628 | 449 ± 49** |
| IP-10 (CXCL-10; pg/ml BAL fluid) | | |
| Day 6 | 500 ± 121 | 100 ± 50* |

[a] BAL, Bronchoaveolar lavage.
*, $p < 0.05$.
** $p < 0.005$.

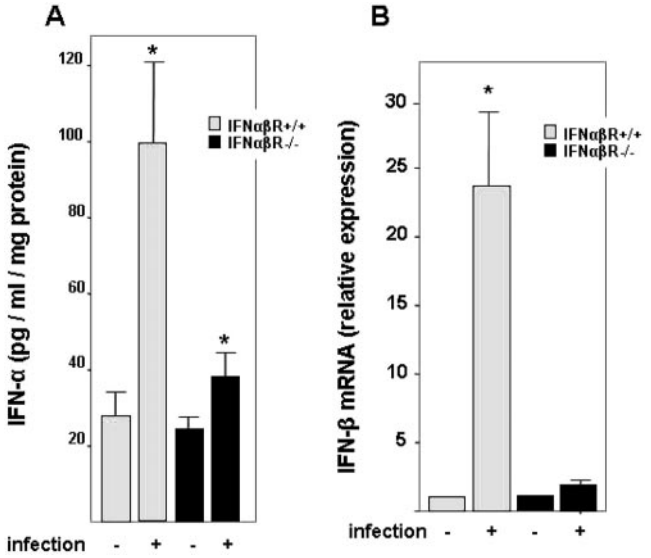


**FIGURE 2.** *A*, Detection of IFN-$\alpha$ (pg/ml/mg lung protein) by ELISA in clarified lung homogenates of mice on day 0 and day 6 postinoculation with 60 PFU PVM ($n = 3$–4 mice per time point; *, $p < 0.05$ vs day 0 of same genotype). *B*, Relative expression of transcripts encoding IFN-$\beta$ detected by Q-RT-PCR in total RNA isolated from whole lungs from mice at time points as above ($n = 4$ mice per time point; *, $p < 0.05$).

### *Identification of transcripts preferentially expressed in PVM-infected, IFN-αβR-deficient mice vs wild type*

In the second half of the gene microarray analysis, we focus on the transcripts preferentially expressed in the IFN-$\alpha\beta R^{-/-}$ mice (Table III; N.B.: this table is organized as wild-type vs IFN-$\alpha\beta R^{-/-}$, and values are shown as negative numbers so as to distinguish them clearly from those presented in Table I). Transcripts that are preferentially expressed in PVM-infected IFN-$\alpha\beta R^{-/-}$ mice are in effect suppressed by one or more aspects of IFN-$\alpha\beta$R-mediated signaling. Most prominent among these IFN-suppressed transcripts are those encoding the CC chemokines eotaxin-2 and TARC (confirmed by Q-RT-PCR and ELISA, respectively; Table IV) and mEar 11 (confirmed by Q-RT-PCR; Fig. 3*A*). Despite its name, mEar 11 is also produced by lung macrophages (30) and belongs to a large cluster of homologous ribonucleases that are produced in response to inflammation (30–32). The 20 ± 3-fold increase in mEar 11 transcript (day 6 postinoculation, infected IFN-$\alpha\beta R^{-/-}$ vs infected wild type) correlates with a ~5-fold increase in mEar protein (Fig. 3*B*) and 3-fold increase in RNase activity (Fig. 3*C*). Although TARC is known as a chemoattractant for Th2 $CD4^+$ cells, and mEar 11 is produced in lung macrophages in response to Th2 stimulus, no elevations in Th2 cytokines IL-4 or IL-5 were detected either on gene microarray or by ELISA (Table IV). This can be contrasted to the findings of Durbin et al. (33) who reported induction of Th2 cytokines in response to respiratory syncytial virus in Stat $1^{-/-}$ mice and concomitant eosinophilic inflammation in lung tissue.

### *Microscopic pathology and analysis of recruited leukocytes*

Examples of characteristic lung pathology of wild-type (IFN-$\alpha\beta R^{+/+}$) and gene-deleted (IFN-$\alpha\beta R^{-/-}$) mice on day 6 postinoculation are shown in Fig. 4. We observe multifocal acute alveolitis with intra-alveolar edema in the parenchymal lung tissue of wild-type mice (Fig. 4, *A* and *C*), with occasional hemorrhage and moderate granulocytic infiltrates throughout. This is accompanied by bronchiolar cell hyperplasia and occasional necrosis of epithelial lining cells. In contrast, the IFN-$\alpha\beta R^{-/-}$-infected mice display a more pronounced multifocal bronchiolitis with infiltration by a mixed population of inflammatory cells (Fig. 4, *B* and *D*). This is also associated with perivascular infiltration with margination of leukocytes frequently appreciated. Edema was not as prominent as in the wild-type infected mice.

Analysis of leukocytes in airways was determined by assessment of bronchoalveolar lavage fluid obtained on day 6 postinoculation. Consistent with the lung pathology observed, 7- to 8-fold fewer leukocytes were recovered from the airways of IFN-$\alpha\beta R^{-/-}$ mice (Table V). Among the recovered leukocytes, we observed an increased proportion of eosinophils (from 3 to 9%) and mononuclear leukocytes (from 4 to 24%) when compared with samples obtained from the wild-type mice.

In each case, a small percentage of the total cells in the BAL fluid samples were $CD3^+$ T cells (wild type, 2.1 ± 0.79%; IFN-$\alpha\beta R^{-/-}$, 2.0 ± 0.41%; $n = 5$; no significant difference). However, the proportions of $CD4^+$ and $CD8^+$ T cells differed significantly (Fig. 5). Among the wild-type mice, 39.1 ± 3.5% of the $CD3^+$ T cells were $CD4^+$, and 40.5 ± 1.7% were $CD8^+$; among the IFN-$\alpha\beta R^{-/-}$ mice, 67.8 ± 3.1% of the $CD3^+$ T cells were $CD4^+$, and 10.3 ± 2.0% were $CD8^+$ ($p < 0.01$; median values presented). These results are consistent with 1) a limited degree of preferential recruitment of $CD4^+$ T cells in response to TARC and eotaxin-2 (given that there were fewer leukocytes overall (Table V)) and/or 2) a defective primary $CD8^+$ T cell response in the IFN-$\alpha\beta R^{-/-}$ mice (34).

Table III. *Differential expression of transcripts comparing pneumovirus-infected wild-type mice vs pneumovirus-infected IFN-αβR gene-deleted mice*[a]

| Accession No. | Gene | Description | Fold Change |
|---|---|---|---|
| Chemokines | | | |
| AF281075 | *CCL-24* | Eotaxin-2 | −11.4* |
| NM_011332 | *CCL-17* | TARC | −3.84* |
| BC012658 | *CCL-22* | MDC | −2.74* |
| Ribonucleases | | | |
| BC020070 | *Ear 11* | Eosinophil-associated ribonuclease 11 | −10.5* |
| Th2 cytokines | | | |
| NM_021283 | *IL-4* | IL-4 | −0.73* |
| NM_010558 | *IL-5* | IL-5 | −2.16* |
| Others | | | |
| AF373412 | *CD209e* | Cell surface Ag | −4.92 |
| AF374470 | *CD209a* | Cell surface Ag | −3.30 |
| AB013898 | *Tnfrsf11b* | Tnf superfamily 11b, osteoprotegerin | −3.09 |

[a] Only values ≥ |2.5| are considered significant. Values denoted by asterisks (*) have been evaluated directly by ELISA (Table 4) or Q-RT-PCR (Fig. 6).

Table IV. *Detection of chemokines eotaxin-2 in lung tissue RNA and TARC, and MDC in lung tissue homogenates of wild-type (IFN-$\alpha\beta R^{+/+}$) and IFN-$\alpha\beta$R gene-deleted mice (IFN-$\alpha\beta R^{-/-}$) in response to infection with PVM (inoculation on day 0 with 60 PFU*

| | IFN-$\alpha\beta R^{+/+}$ | | IFN-$\alpha\beta R^{-/-}$ | |
|---|---|---|---|---|
| Eotaxin-2 (relative expression) | | | | |
| | Uninfected | PVM-infected | Uninfected | PVM-infected |
| Day 6 | 1.0 | 0.4 ± 0.01 | 2.0 ± 0.05 | 9.0 ± 3* |
| TARC (CCL-17; pg/ml/mg lung homogenate protein) | | | | |
| Day 0 | | 57 ± 7.4 | | 56 ± 11 |
| Day 4 | | 323 ± 13 | | 586 ± 19** |
| Day 6 | | 543 ± 71 | | 1040 ± 297* |
| TARC (CCL-17; pg/ml BAI[a] fluid) | | | | |
| Day 6 | | 150 ± 33 | | 1000 ± 131** |
| MDC (CCL-22; pg/ml/mg lung homogenate protein) | | | | |
| Day 4 | | 183 ± 31 | | 195 ± 48 |
| Day 6 | | 538 ± 40 | | 381 ± 136 |
| IL-4 (pg/ml/mg lung homogenate protein) | | | | |
| Day 6 | | 0 | | 0 |
| IL-5 (pg/ml/mg lung homogenate protein) | | | | |
| Day 6 | | 0 | | 0 |

[a] BAL, broachoalveolar fluid.
*, $p < 0.05$.
**, $p < 0.005$.

### *Production of antiviral chemokines MIP-1α and MIP-2*

Given the differential recruitment of leukocytes in response to PVM, we considered the possible contribution of the chemokines MIP-1$\alpha$ and/or MIP-2, despite the absence of evidence of differential expression on gene microarray (Table I). In our previous work, we have demonstrated local production of the CC chemokine MIP-1$\alpha$ and the CXC chemokine MIP-2 in response to PVM infection (23, 35). Although MIP-1$\alpha$-mediated inflammatory response blocks virus replication, and CCR1 gene-deleted mice tend to survive somewhat longer in response to moderate virus inocula (23), in the end, the negative sequelae of the MIP-1$\alpha$-mediated inflammatory response are clearly in evidence. Furthermore, we have shown that genetic and/or biochemical blockade of MIP-1$\alpha$ or its receptor, CCR1, eliminates the granulocytic inflammatory response characteristic of this infection (19, 20). As shown in Tables I and III, we observed no differential expression of transcripts encoding MIP-1$\alpha$ or of MIP-2 on gene microarray. Furthermore, both chemokines were detected in mouse lung homogenates, but no differential expression was observed (Table VI). Thus, neither MIP-1$\alpha$ nor MIP-2 expression can explain the differential pathology observed between the wild-type and IFN-$\alpha\beta R^{-/-}$ gene-deleted strains of mice in response to PVM infection.

### *Virus replication in wild-type vs IFN-$\alpha\beta R^{-/-}$ mice*

Virus replication was determined qualitatively by Western blotting of clarified lung homogenates probed with rabbit polyclonal anti-PVM N nucleoprotein (Fig. 6*A*) and quantitatively by Q-RT-PCR of lung RNA from PVM-infected wild-type (IFN-$\alpha\beta R^{+/+}$) and gene-deleted (IFN-$\alpha\beta R^{-/-}$) mice (Fig. 6*B*). The Western blot demonstrates a time-dependent increase in intensity of the band representing PVM N protein with increased intensity on days 3–5 postinoculation among the IFN-$\alpha\beta R^{-/-}$ mice. Q-RT-PCR was performed to determine a more precise copy number, using the SH transcript as a target. No virus RNA was detected in mice before inoculation (Fig. 5*B*) or directly after inoculation with 60 PFU (data not shown). Virus recovery on day 6 was 3.0 ± 1.4 × $10^4$

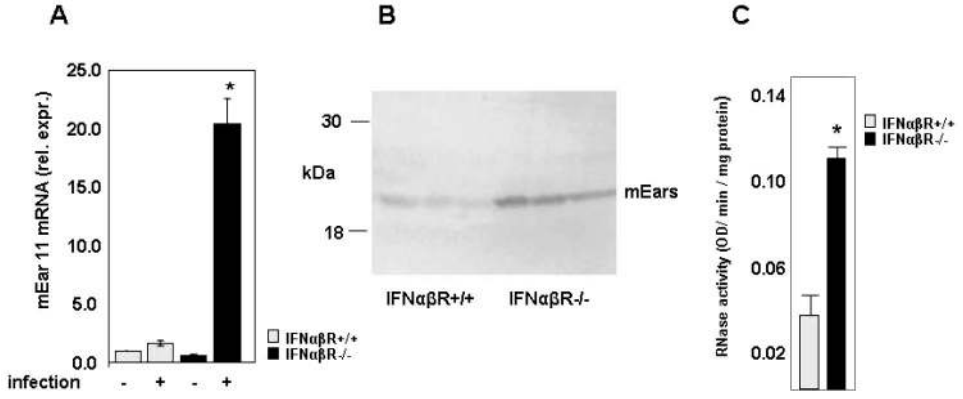


**FIGURE 3.** *A*, Relative expression of transcripts encoding mEar 11 by Q-RT-PCR in total RNA isolated from whole mouse lung from wild-type IFN-$\alpha\beta R^{+/+}$ and gene-deleted IFN-$\alpha\beta R^{-/-}$ mice on day 6 postinoculation ($n = 4$–5 mice per time point). Asterisk (*) denotes statistically significant differences between datapoint indicated and others shown (*, $p < 0.01$). *B*, Western blot of clarified lung tissue homogenate from wild-type IFN-$\alpha\beta R^{+/+}$ and gene-deleted IFN-$\alpha\beta R^{-/-}$ mice. Blot containing homogenate (30 $\mu$g) is probed with rabbit polyclonal anti-mEars Ab, documenting a 5.5 ± 0.4-fold increase in mEar expression in expression. *C*, RNase activity in clarified homogenates, determined as acid soluble ribonucleotides generated from acid-insoluble tRNA per unit time per microgram lung tissue as described in *Materials and Methods* ($n = 3$ mice per point). Asterisk (*) denotes statistically significant differences ($p < 0.01$) between genotypes.

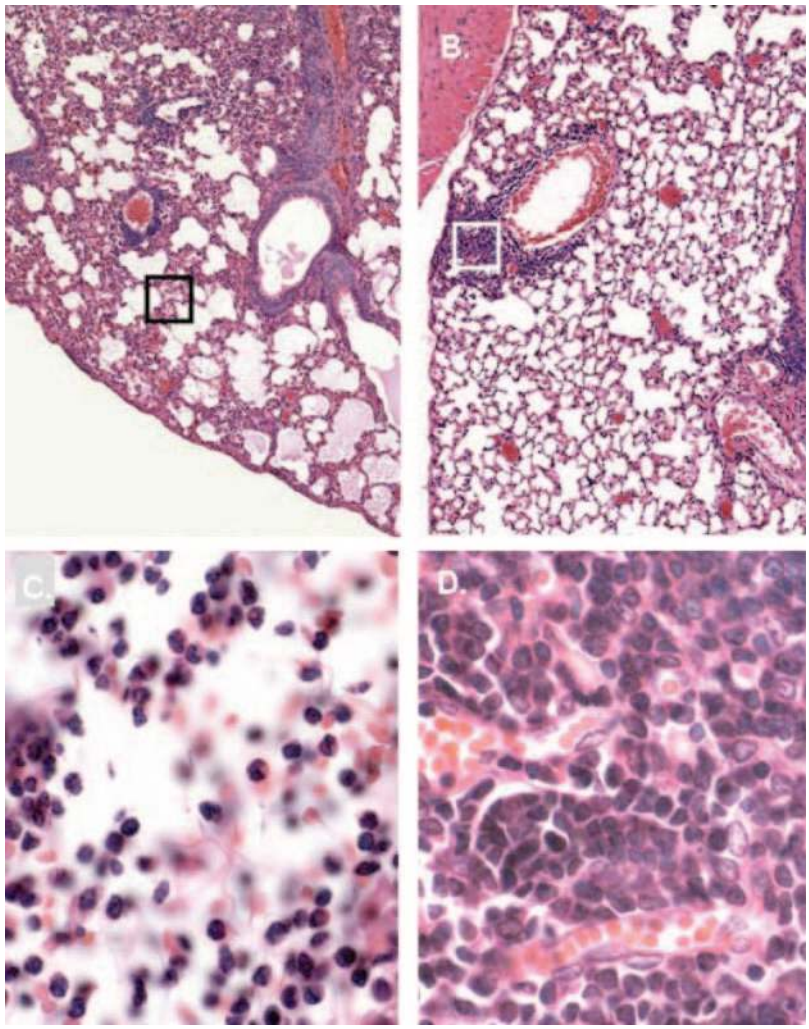


**FIGURE 4.** Microscopic histology of lung tissue from wild-type IFN-$\alpha\beta R^{+/+}$ (*A* and *C* at original magnifications ×20 and ×63, respectively) and gene-deleted IFN-$\alpha\beta R^{-/-}$ (*B* and *D* at original magnifications ×20 and ×63, respectively) mice sacrificed on day 6 postinoculation. Regions in boxes in *A* and *C* are expanded in *B* and *D*, respectively, as shown.

copies/$\mu$g lung RNA from wild-type mice, and $9.5 \pm 1.2 \times 10^4$ copies/$\mu$g lung RNA for the IFN-$\alpha\beta R^{-/-}$ mice (*, $p < 0.05$).

### *Differential survival*

A total of 30 age- (±3 days) and gender-matched wild-type (IFN-$\alpha\beta R^{+/+}$) and gene-deleted (IFN-$\alpha\beta R^{-/-}$) mice (15 per genotype) were compared for survival analysis (Fig. 6*C*). The first deaths occurred on day 7 postinoculation, which were two of the wild-type group; the wild-type group reached 100% mortality by day 12, with 50% survival calculated at 9.0 ± 0.3 days. In contrast, the first death among the gene-deleted (IFN-$\alpha\beta R^{-/-}$) mice did not occur until day 8, and the group included one long-term survivor (regained lost weight and maintained vigor through day 40, seroconversion documented). Using day 18 as the cutoff for the long-term survivor, 50% survival of the IFN-$\alpha\beta R^{-/-}$ mice was calculated at 10.8 ± 0.6 days ($p < 0.02$). Thus, the IFN-$\alpha\beta R^{-/-}$ mice have a clear survival advantage over their wild-type counterparts. Although seemingly paradoxical, we know from previous work that the inflammatory response to pneumovirus infection plays a crucial role in this infection (19, 20). It is likely that differential activation of the inflammatory response accounts for the paradoxical survival observed here.

Table V. *Detection and identification of leukocytes in BAL[a] fluid of wild-type (IFN-$\alpha\beta R^{+/+}$) and IFN-$\alpha\beta R$ gene-deleted mice*

| | |
|---|---|
| Wild-type (IFN-$\alpha\beta R^{+/+}$) | $3.2 \pm 0.7 \times 10^5$ leukocytes/ml BAL fluid |
| Neutrophils | 93.0 ± 2.0% |
| Eosinophils | 3.0 ± 1.2% |
| Monocytes | 3.9 ± 0.6% |
| Lymphocytes | 0.45 ± 0.45% |
| Gene-deleted (IFN-$\alpha\beta R^{-/-}$) | $0.45 \pm 0.03 \times 10^5$ leukocytes/ml BAL fluid |
| Neutrophils | 67.0 ± 4.6%* |
| Eosinophils | 9.2 ± 2.8%* |
| Monocytes | 15.0 ± 2.6%* |
| Lymphocytes | 8.5 ± 2.3%* |

[a] BAL, bronchoalveolar fluid.
*, $p < 0.05$.

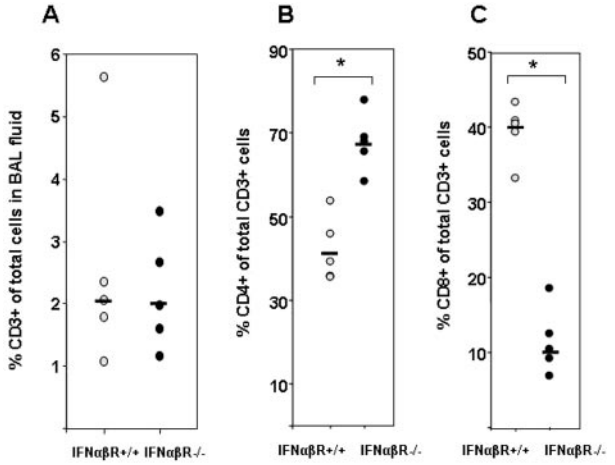


**FIGURE 5.** Flow cytometric analysis of bronchoalveolar lavage fluid from wild-type (IFN-αβR$^{+/+}$) and IFN-αβR$^{-/-}$ mice ($n = 5$ per genotype) on day 6 postinoculation. *A*, Percentage cells expressing CD3$^+$ Ag; *B*, percentage of CD4$^+$ cells of total CD3$^+$ T cells; and *C*, percentage CD8$^+$ cells of total CD3$^+$ T cells. Horizontal bar, median value; ∗, $p < 0.01$.

Table VI. *Detection of chemokines MIP-1α and MIP-2 in lung tissue homogenates of wild-type (IFN-αβR$^{+/+}$) and IFN-αβR gene-deleted mice (IFN-αβR$^{-/-}$) in response to infection with PVM (inoculation on day 0 with 60 PFU)*

| | IFN-αβR$^{+/+}$ | IFN-αβR$^{-/-}$ |
|---|---|---|
| MIP-1α (pg/ml/mg lung homogenate protein) | | |
| Day 0 | 0 | 0 |
| Day 5 | 109 ± 26 | 108 ± 20 |
| Day 6 | 180 ± 63 | 136 ± 23 |
| MIP-1α (pg/ml BAL[a] fluid) | | |
| Day 6 | 12 ± 3.2 | 5.0 ± 1.6 |
| MIP-2 (pg/ml/mg lung homogenate protein) | | |
| Day 0 | 0 | 6 ± 0.7 |
| Day 4 | 114 ± 18 | 111 ± 3.1 |
| Day 5 | 530 ± 190 | 376 ± 89 |
| Day 6 | 107 ± 12 | 129 ± 19 |
| MIP-2 (pg/ml BAL fluid) | | |
| Day 6 | 51 ± 11 | 50 ± 6.8 |

[a] BAL, bronchoalveolar fluid.

## Discussion

Via a gene microarray comparison between wild-type (IFN-αβR$^{+/+}$) and IFN-αβR-deficient (IFN-αβR$^{-/-}$) mice, we demonstrate receptor-dependent transcriptional activation of many of the classic IFN response genes, including those of the antiviral cascade (multiple Oas genes, PRKR, Mx1). PVM replication in vivo was clearly diminished by the actions of the IFN response genes, demonstrating the fact that pneumoviruses are not resistant to the effects of endogenous type I IFNs in vivo. Molecular dissection of the bRSV and hRSV pathogens has suggested a role for the nonstructural NS-1 and NS-2 proteins (7–10) in antagonizing the activities of the IFN-mediated antiviral proteins. However, Mohapatra and colleagues (36) have recently demonstrated that administration of small interfering RNA silencing respiratory syncytial virus NS1 expression results in reduced virus replication both in tissue culture and in vivo. Further RNA silencing and/or reverse genetics approaches might provide insight into the roles of the PVM nonstructural NS-1 and NS-2 proteins and their interactions with the IFN-mediated antiviral state.

We observe a small but significant survival differential, which, seemingly paradoxically, proves to be advantageous for the gene-deleted IFN-αβR$^{-/-}$ mice. This might be puzzling were it not for our earlier observations on the crucial contributions of the antiviral inflammatory responses associated with this disease (19, 20, 23). The microscopic pathology suggested distinct differences in the nature of the antiviral inflammatory response among the wild-type (IFN-αβR$^{+/+}$) and gene-deleted (IFN-αβR$^{-/-}$) mice, the former

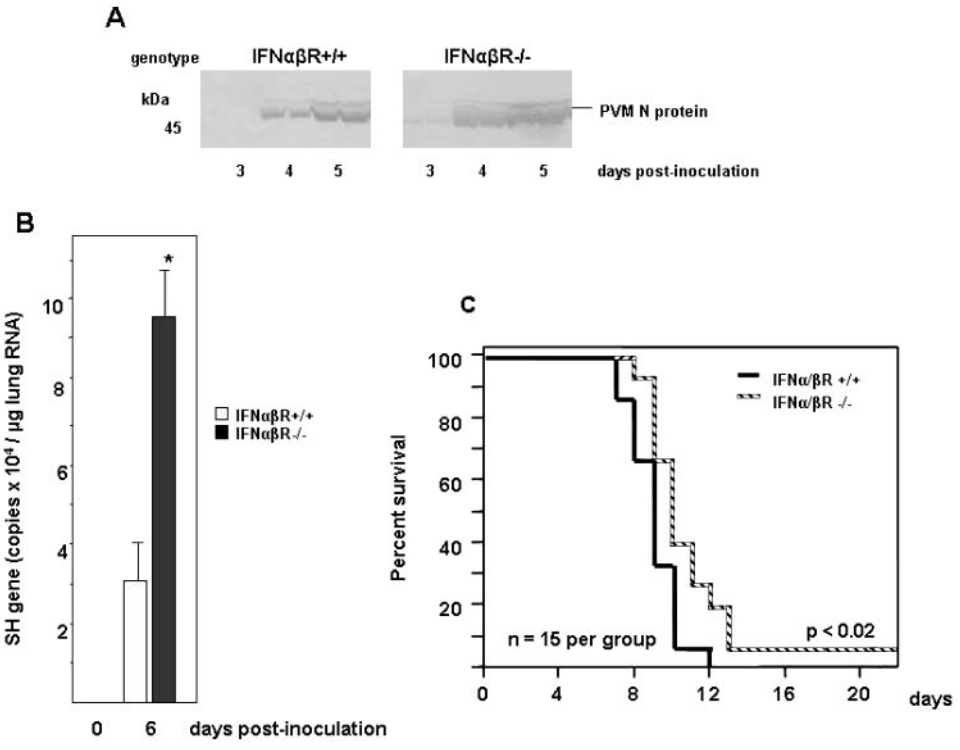


**FIGURE 6.** *A*, Western blot of clarified lung homogenates from wild-type IFN-αβR$^{+/+}$ and gene-deleted IFN-αβR$^{-/-}$ mice sacrificed on days 3–5 postinoculation. Blot is probed with rabbit polyclonal anti-PVM N protein. *B*, Detection of PVM SH gene transcripts in whole lung RNA from IFN-αβR$^{+/+}$ and IFN-αβR$^{-/-}$ mice; $n = 4$ mice per time point; ∗, $p < 0.05$. *C*, Survival of wild-type IFN-αβR$^{+/+}$ and gene-deleted IFN-αβR$^{-/-}$ mice. Statistically significant increased survival (∗, $p < 0.02$) was observed among the IFN-αβR$^{-/-}$ gene-deleted mice; the survivor regained lost weight and was maintained through t = 40 days; confirmed as infected via seroconversion.

characterized by a more edematous pattern with neutrophils predominating, and the latter, one with an overall reduced inflammatory response, and preferential recruitment of eosinophils and mononuclear leukocytes. The chemokine MIP-1$\alpha$, which elicits primarily neutrophils, is not differentially expressed in wild-type vs IFN-$\alpha\beta R^{-/-}$ mice, but we do observe reduced expression of the chemokines monocyte chemotactic protein-5 and IP-10 and preferential expression of eotaxin-2 (CCL-24), TARC (CCL-17), and the proinflammatory enzyme mEar 11 in IFN-$\alpha\beta R^{-/-}$ gene-deleted mice. Eotaxin-2 is a chemoattractant for eosinophils (37), and TARC, for T cells, primarily memory effector $CD4^+$, with a preference for Th2 cells (38). Mouse Ear11 is a member of the highly divergent mouse ribonuclease cluster that is orthologous to the eosinophil-derived neurotoxin/RNase 2 gene of the RNase A superfamily. The RNase A superfamily is a highly divergent, multilineage enzyme family that is unique to vertebrate species (39). Despite its name, mEar 11 is found not only in eosinophils, but in lung macrophages in response to allergic (Th2) stimuli (30) (although we observed no Th2 cytokines present in lung tissue in response to this infection model; see Table IV). Mouse Ear 11 is absent at homeostasis, but has been detected in response to allergic, biochemical, and now microbial provocation in lung tissue. Among its potential functions, the paralogous gene, mEar 2, is a chemoattractant for mouse dendritic cells in vitro and in vivo (40), and related RNase A ribonucleases have antiviral activity in vitro (41).

The apparent differences in cellular recruitment are particularly intriguing, given the complex nature of the inflammatory response to this infection. It would be interesting to elucidate the signals that elicit the cellular inflammatory responses in the IFN-$\alpha\beta R^{-/-}$ mice, and to determine what the unique relationship there might be between IFN-$\alpha\beta$R-mediated signaling and the differential control of cellular inflammation. Based on the chemoattractant properties, the differential expression of these mediators may be causally associated with the recruitment of eosinophils and mononuclear leukocytes, and/or the differential recruitment/responses of T cell subsets observed among IFN-$\alpha\beta R^{-/-}$-infected mice.

Although future work will define the relationships of these transcripts and their protein products to the inflammatory response observed in the IFN-$\alpha\beta R^{-/-}$ mice, as a group, they represent a novel set of IFN-suppressed genes, or transcripts expressed in response to virus infection only in the absence of IFN-$\alpha\beta$R-mediated signaling. There are other examples of interactions between type I IFN signaling and innate/acquired immunity–specifically, induction of MHC I (41, 42) and RANTES (11–13), but in direct response to IFN-$\beta$ and IRF-3, respectively. In the situation here, expression of atypical proinflammatory genes correlates with improved survival in the setting of an otherwise fatal pneumovirus infection in IFN-$\alpha\beta R^{-/-}$ mice. Of particularly intriguing interest–how might expression genes that would otherwise be suppressed in the presence of an intact IFN-signaling mechanism, particularly proinflammatory mediators, alter the disease outcomes in infections caused by viruses that have acquired the ability to antagonize IFN production and/or signaling at the receptor? Our work suggests an unexplored interaction between IFN receptor-mediated signaling and the antiviral inflammatory response that can now be dissected at the molecular level.

Of perhaps even greater interest–how can we exploit these findings to develop novel anti-inflammatory therapies for severe respiratory infections? Using the PVM as a model for the more severe forms of hRSV, we have already shown that the use of antivirals alone is insufficient, and only when antivirals are coupled with anti-inflammatory (or, more specifically, carefully crafted immunomodulatory therapy directed against the chemokine MIP-1$\alpha$ and/or its receptor CCR1) can we alter the course of disease and effect significant reductions in morbidity and mortality (reviewed in Ref. 35). From this work, we observe that an alteration of the inflammatory milieu–including overexpression of the cytokines TARC, eotaxin-2, and potentially mEar11, and/or reduced expression of monocyte chemotactic protein-5 and IP-10–may alter the course of an otherwise fatal pneumonia by altering the nature of the inflammatory response. This warrants further exploration from a therapeutic perspective.

## Acknowledgments

We thank Dr. Wolfgang Leitner (National Cancer Institute, Bethesda, MD) for the original heterozygote IFN-$\alpha\beta R^{+/-}$ mice on the C57BL/6 background, Drs. James Lee and Nancy Lee (Mayo Clinic, Scottsdale, AZ) for the anti-mEars polyclonal Ab, Dr. Andrew Brooks (Functional Genomics Center, Rochester, NY) for executing the gene microarray experiments, and the staff of the Building 14BS animal facility (National Institute of Allergy and Infectious Diseases) for care of the mice used in these experiments.

## Disclosures

The authors have no financial conflict of interest.

## References

1. Sarkar, S. N., and G. C. Sen. 2004. Novel functions of proteins encoded by viral stress-inducible genes. *Pharmacol. Ther.* 103: 245–259.
2. Malmgaard, L. 2004. Induction and regulation of IFNs during viral infections. *J. Interferon Cytokine Res.* 24: 439–454.
3. Gotoh, B., T. Komatsu, K. Takeuchi, and J. Yokoo. 2001. Paramyxovirus accessory proteins as interferon antagonists. *Microbiol. Immunol.* 45: 787–800.
4. Gotoh, B., T. Komatsu, K. Takeuchi, and J. Yokoo. 2002. Paramyxovirus strategies for evading the interferon response. *Rev. Med. Virol.* 12: 337–357.
5. Horvath, C. M. 2004. Silencing STATs: lessons from paramyxovirus interferon evasion. *Cytokine Growth Factor Rev.* 15: 117–127.
6. Young, D. F., L. Didcock, S. Goodbourn, and R. E. Randall. 2000. *Paramyxoviridae* use distinct virus-specific mechanisms to circumvent the interferon response. *Virology* 269: 383–390.
7. Bossert, B., and K. K. Conzelmann. 2002. Respiratory syncytial virus (RSV) nonstructural proteins as host range determinants: a chimeric bovine RSV with NS genes from human RSV is attenuated in interferon-competent bovine cells. *J. Virol.* 76: 4287–4293.
8. Schlender, J., B. Bossert, U. Buchholz, and K. K. Conzelmann. 2000. Bovine respiratory syncytial virus nonstructural proteins NS1 and NS2 cooperatively antagonize $\alpha/\beta$ interferon-induced antiviral response. *J. Virol.* 74: 8232–8242.
9. Spann, K. M., K. C. Tran, B. Chi, R. L. Rabin, and P. L. Collins. 2004. Suppression of the induction of $\alpha$, $\beta$, and $\lambda$ interferons by the NS1 and NS2 proteins of human respiratory syncytial virus in human epithelial cells and macrophages. *J. Virol.* 78: 4363–4369.
10. Valarcher, J. F., J. Furze, S. Wyld, R. Cook, K. K. Conzelmann, and G. Taylor. 2003. Role of $\alpha/\beta$ interferons in the attenuation and immunogenicity of recombinant bovine respiratory syncytial viruses lacking NS proteins. *J. Virol.* 77: 8426–8439.
11. Genin, P., M. Algarte, P. Roof, R. Lin, and J. Hiscott. 2000. Regulation of RANTES chemokine gene expression requires cooperativity between NF-$\kappa$B and IFN-regulatory factor transcription factors. *J. Immunol.* 164: 5352–5361.
12. Lin, R., C. Heylbroeck, P. Genin, P. M. Pitha, and J. Hiscott. 1999. Essential role of interferon regulatory factor 3 in direct activation of RANTES chemokine transcription. *Mol. Cell. Biol.* 19: 959–966.
13. Casola, A., R. P. Garofalo, H. Haeberle, T. F. Elliott, R. Lin, M. Jamaluddin, and A. R. Brasier. 2001. Multiple *cis* regulatory elements control RANTES promoter activity in alveolar epithelial cells infected with respiratory syncytial virus. *J. Virol.* 75: 6428–6439.
14. Grandvaux, N., M. J. Servant, B. tenOever, G. C. Sen, S. Balachandran, G. N. Barber, R. Lin, and J. Hiscott. 2002. Transcriptional profiling of interferon regulatory factor 3 target genes: direct involvement in the regulation of interferon-stimulated genes. *J. Virol.* 76: 5532–5539.
15. Barnes, B. J., J. Richards, M. Mancl, S. Hanash, L. Beretta, and P. M. Pitha. 2004. Global and distinct targets of IRF-5 and IRF-7 during innate response to viral infection. *J. Biol. Chem.* 279: 45194–45207.
16. Hokeness, K. L., W. A. Kuziel, C. A. Biron, and T. P. Salazar-Mather. 2005. Monocyte chemoattractant protein-1 and CCR2 interactions are required for IFN-$\alpha\beta$-induced inflammatory responses and antiviral defense in liver. *J. Immunol.* 174: 1549–1556.
17. Salazar-Mather, T. P., C. A. Lewis, and C. A. Biron. 2002. Type I interferons regulate inflammatory cell trafficking and macrophage inflammatory protein-1$\alpha$ delivery to the liver. *J. Clin. Invest.* 110: 321–330.
18. Salazar-Mather, T. P., T. A. Hamilton, and C. A. Biron. 2000. A chemokine-to-cytokine-to-chemokine cascade critical in antiviral defense. *J. Clin. Invest.* 105: 985–993.

19. Bonville, C. A., A. J. Easton, H. F. Rosenberg, and J. B. Domachowske JB. 2003. Altered pathogenesis of severe pneumovirus infection in response to combined anti-viral and specific immunomodulatory agents. *J. Virol.* 77: 1237–1244.
20. Bonville, C. A., V. Lao, J. M. DeLeon, J. L. Gao, A. J. Easton, H. F. Rosenberg, and J. B. Domachowske. 2004. Functional antagonism of chemokine receptor CCR1 reduces mortality in acute pneumovirus infection in vivo. *J. Virol.* 78: 7984–7989.
21. Barends, M., L. G. de Rond, J. Dormans, M. van Oosten, A. Boelen, H. J. Neijens, A. D. Osterhaus, and T. G. Kimman. 2004. Respiratory syncytial virus, pneumonia virus of mice, and influenza A virus differently affect respiratory allergy in mice. *Clin. Exp. Allergy* 34: 488–496.
22. Muller, U., U. Steinhoff, L. F. Reis, S. Hemmi, J. Pavlovic, R. M. Zinkernagel, and M. Aguet. 1994. Functional role of type I and type II interferons in antiviral defense. *Science* 264: 1918–1921.
23. Domachowske, J. B., C. A. Bonville, J. L. Gao, P. M. Murphy, A. J. Easton, and H. F. Rosenberg. 2000. The chemokine MIP-1$\alpha$ and its receptor CCR1 control pulmonary inflammation and anti-viral host defense in paramyxovirus infection. *J. Immunol.* 165: 2677–2682.
24. Domachowske, J. B., C. A. Bonville, A. J. Easton, and H. F. Rosenberg. 2002. Differential expression of pro-inflammatory cytokine genes in vivo in response to pathogenic and non-pathogenic pneumovirus infection. *J. Infect. Dis.* 186: 8–14.
25. Rosenberg, H. F., and J. B. Domachowske. 2001. Eosinophil-derived neurotoxin. In *Methods in Enzymology.* A. W. Nicholson, ed. Academic Press, San Diego, p. 273–286.
26. Heinz, S., V. Haehnel, M. Karaghiosoff, L. Schwarzfischer, M. Muller, S. W. Krause, and M. Rehli. 2003. Species-specific regulation of Toll-like receptor 3 genes in men and mice. *J. Biol. Chem.* 278: 21502–21509.
27. Ritchie, K. J., C. S. Hahn, K. I. Kim, M. Yan, D. Rosario, L. Li, J. C. de la Torre, and D. E. Zhang. 2004. Role of ISG15 protease UBP43 (USP18) in innate immunity to viral infection. *Nat. Med.* 10: 1374–1378.
28. Rudd, B. D., E. Burstein, C. S. Duckett, X. Li, and N. W. Lukacs. 2005. Differential role for TLR3 in respiratory syncytial virus-induced chemokine expression. *J. Virol.* 79: 3350–3357.
29. Malmgaard, L., T. P. Salazar-Mather, C. A. Lewis, and C. A. Biron. 2002. Promotion of $\alpha/\beta$ interferon induction during in vivo viral infection through $\alpha/\beta$ interferon receptor/STAT1 system-dependent and -independent pathways. *J. Virol.* 76: 4520–4525.
30. Cormier, S. A., S. Yuan, J. R. Crosby, C. A. Protheroe, D. M. Dimina, E. M. Hines, N. A. Lee, and J. J. Lee. 2002. $T_H2$-mediated pulmonary inflammation leads to the differential expression of ribonuclease genes by alveolar macrophages. *Am. J. Respir. Cell Mol. Biol.* 27: 678–687.
31. Larson, K. A., E. V. Olson, B. J. Madden, G. J. Gleich, N. A. Lee, and J. J. Lee. 1996. Two highly homologous ribonuclease genes expressed in mouse eosinophils identify a larger subgroup of the mammalian ribonuclease superfamily. *Proc. Natl. Acad. Sci. USA* 93: 12370–12375.
32. Zhang, J., K. D. Dyer, and H. F. Rosenberg. 2000. Evolution of the rodent eosinophil-associated ribonuclease gene family by rapid gene sorting and positive selection. *Proc. Natl. Acad. Sci. USA* 97: 4701–4706.
33. Durbin, J. E., T. R. Johnson, R. K. Durbin, S. E. Mertz, R. A. Morotti, R. S. Peebles, and B. S. Graham. 2002. The role of IFN in respiratory syncytial virus pathogenesis. *J. Immunol.* 168: 2944–2952.
34. Pien, G. C., K. B. Nguyen, L. Malmgaard, A. R. Satoskaar, and C. A. Biron. 2002. A unique mechanism for innate cytokine promotion of T cell responses to viral infections. *J. Immunol.* 169: 5827–5837.
35. Rosenberg, H. F., C. A. Bonville, A. J. Easton, and J. B. Domachowske. 2004. The pneumonia virus of mice (PVM) infection model for severe respiratory syncytial virus infection: identifying novel targets for therapeutic intervention. *Pharmacol. Ther.* 105: 1–16.
36. Zhang, W., H. Yang, S., Kong, S. Mohapatra, H. San Juan-Vergara, G. Hellermann, S. Behera, R. Singam, R. F. Lockey, and S. S. Mohapatra. 2005. Inhibition of respiratory syncytial virus infection with intranasal siRNA nanoparticles targeting the viral NS1 gene. *Nat. Med.* 11: 56–62.
37. Lampinen, M., M. Carlson, L. D. Hakansson, and P. Venge. 2004. Cytokine-regulated accumulation of eosinophils in inflammatory disease. *Allergy* 59: 793–805.
38. Yoshie, O., T. Imai, and H. Nomiyama. 1997. Novel lymphocyte-specific CC chemokines and their receptors. *J. Leukocyte Biol.* 62: 634–644.
39. Beintema, J. J. 1998. Introduction: the ribonuclease A superfamily. *Cell Mol. Life Sci.* 54: 763–765.
40. Yang, D., H. F. Rosenberg, Q. Chen, K. D. Dyer, K. Kurosaka, and J. J. Oppenheim. 2003. Eosinophil-derived neurotoxin (EDN), an antimicrobial protein with chemotactic activity for dendritic cells. *Blood* 102: 3396–3404.
41. Domachowske, J. B., K. D. Dyer, C. A. Bonville, and H. F. Rosenberg. 1998. Recombinant human eosinophil-derived neurotoxin/RNase 2 functions as an effective antiviral agent against respiratory syncytial virus. *J. Infect. Dis.* 177: 1458–1464.
42. Garofalo, R., F. Mei, R. Espejo, G. Ye, H. Haeberle, S. Baron, P. L. Ogra, and V. E. Reyes. 1996. Respiratory syncytial virus infection of human respiratory epithelial cells up-regulates class I MHC expression through the induction of IFN-$\beta$ and IL-1$\alpha$. *J. Immunol.* 157: 2506–2513.